Accepted Manuscript

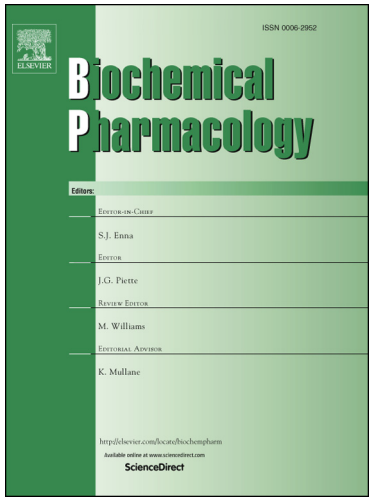

Impaired Thromboxane Receptor Dimerization Reduces Signaling Efficiency: A Potential Mechanism For Reduced Platelet Function In Vivo

Valérie Capra, Mario Mauri, Francesca Guzzi, Marta Busnelli, Maria Rosa Accomazzo, Pascale Gaussem, Shaista P. Nisar, Stuart J. Mundell, Marco Parenti, G. Enrico Rovati

PII: S0006-2952(16)30397-5
DOI: http://dx.doi.org/10.1016/j.bcp.2016.11.010
Reference: BCP 12678

To appear in: *Biochemical Pharmacology*

Received Date: 31 August 2016
Accepted Date: 10 November 2016

Please cite this article as: V. Capra, M. Mauri, F. Guzzi, M. Busnelli, M. Rosa Accomazzo, P. Gaussem, S.P. Nisar, S.J. Mundell, M. Parenti, G. Enrico Rovati, Impaired Thromboxane Receptor Dimerization Reduces Signaling Efficiency: A Potential Mechanism For Reduced Platelet Function In Vivo, *Biochemical Pharmacology* (2016), doi: http://dx.doi.org/10.1016/j.bcp.2016.11.010

Impaired Thromboxane Receptor Dimerization Reduces Signaling Efficiency: A Potential Mechanism For Reduced Platelet Function In Vivo

Valérie Capra[a,b*], Mario Mauri[c*], Francesca Guzzi[c], Marta Busnelli[d,e], Maria Rosa Accomazzo[a], Pascale Gaussem[f], Shaista P. Nisar[g], Stuart J. Mundell[g], Marco Parenti[c], G. Enrico Rovati[a]

[a]From the Department of Pharmacological and Biomolecular Sciences and [b]Department of Health Science, University of Milan, Milano, Italy. E-mail addresses: Valerie.Capra@unimi.it, Genrico.Rovati@unimi.it, Maria.Accomazzo@unimi.it

[c]Department of Medicine and Surgery, University of Milano-Bicocca, Monza, Italy. E-mail addresses: mario.mauri@unimib.it, francesca.guzzi@unimib.it, marco.parenti@unimib.it

[d]CNR, Institute of Neuroscience and [e]Department of Medical Biotechnology and Translational Medicine, University of Milan, Milan, Italy. E-mail address: m.busnelli@in.cnr.com

[f]Inserm UMR S765, Faculte´ de Pharmacie, Paris; Université Paris Descartes, and AP-HP, Hopital Européen Georges Pompidou, Service d'Hématologie Biologique, Paris, France. E-mail address: pascale.gaussem@univ-paris5.fr

[g]School of Physiology and Pharmacology, University of Bristol, Bristol, BS8 1TD, UK. E-mail addresses: shaista.nisar@bristol.ac.uk, s.j.mundell@bristol.ac.uk

* These two authors equally contributed to the paper

Corresponding author:
G.Enrico Rovati, Department of Pharmacological and Biomolecular Sciences,
University of Milan, Via Balzaretti 9, 20133 Milano, Italy Tel.: (+39) 0250318369;
E-mai: Genrico.Rovati@unimi.it

ABSTRACT

Thromboxane A_2 is a potent mediator of inflammation and platelet aggregation exerting its effects through the activation of a G protein-coupled receptor (GPCR), termed TP. Although the existence of dimers/oligomers in Class A GPCRs is widely accepted, their functional significance still remains controversial. Recently, we have shown that TPα and TPβ homo-/hetero-dimers interact through an interface of residues in trans-membrane domain 1 (TM1) whose disruption impairs dimer formation. Here, biochemical and pharmacological characterization of this dimer deficient mutant (DDM) in living cells indicates a significant impairment in its response to agonists. Interestingly, two single loss-of-function TPα variants, namely W29C and N42S recently identified in two heterozygous patients affected by bleeding disorders, match some of the residues mutated in our DDM. These two naturally occurring variants display a reduced potency to TP agonists and are characterized by impaired dimer formation in transfected HEK-293T cells. These findings provide proofs that lack of homo-dimer formation is a crucial process for reduced TPα function in vivo, and might represent one molecular mechanism through which platelet TPα receptor dysfunction affects the patient(s) carrying these mutations.

Keywords: G protein coupled receptors; Thromboxane A_2; Signal transduction; Receptor dimer; Platelets; Eicosanoids.

Chemical compounds studied in this article:

U46619 (PubChem CID: 5311493); (Z)-7-[(1S,2S,3R,4R)-3-[(E,3S)-3-hydroxyoct-1-enyl]-5-oxabicyclo[2.2.1]heptan-2-yl]hept-5-enoic acid;

I-BOP (PubChem CID: 51015454); (Z)-7-[(1S,2S,3S,4R)-3-[(E,3R)-3-hydroxy-4-(4-iodophenoxy)but-1-enyl]-7-oxabicyclo[2.2.1]heptan-2-yl]hept-5-enoic acid;

Pinane Thromboxane A2 (PTA2) (PubChem CID: 25834471); (Z)-7-[(1S,3R,4R,5S)-3-[(E,3R)-3-hydroxyoct-1-enyl]-6,6-dimethyl-4-bicyclo[3.1.1]heptanyl]hept-5-enoic acid; SQ29,548 (PubChem CID: 6437074); (Z)-7-[(1R,2R,3R,4S)-3-[[2-(phenylcarbamoyl)hydrazinyl]methyl]-7-oxabicyclo[2.2.1]heptan-2-yl]hept-5-enoic acid; Ramatroban (PubChem CID: 123879); 3-[(3R)-3-[(4-fluorophenyl)sulfonylamino]-1,2,3,4-tetrahydrocarbazol-9-yl]propanoic acid.

1. INTRODUCTION

The completion of the human genome project identified 7 transmembrane receptors, commonly referred to as G protein-coupled receptors (GPCRs), as the widest gene family [1]. Among the five different subfamilies, the Class A or rhodopsin-like GPCRs, to which the thromboxane A_2 receptor (TP) belongs, is the largest [2]. Members of this receptor family exert a wide variety of physiological processes with alterations in GPCR function contributing to the development of a number of pathological processes. Consequently, more than 30% of the current marketed drugs target GPCRs [3], with ongoing efforts to identify new molecules targeting the function of these proteins.

Membrane receptors from other families have long been known to form multimeric complexes, including members of the growth factor receptor family [4]. Conversely, for a long time GPCRs were considered to function as monomeric entities with their activation resulting from the stoichiometric binding of one receptor moiety to a single heterotrimeric G protein. Indeed, a number of biochemical and biophysical data are consistent with the ability of rhodopsin [5-7], or other GPCRs [8-10] to activate their cognate G proteins in a monomeric form. However, pharmacological data from various GPCRs are not compatible with such a model, and increasing evidence suggests that these receptors exist and function as

oligomeric complexes of two or more protomers [11]. Although controversial until a few years ago, the formation of GPCR dimers/oligomers has now been demonstrated not only in ectopically transfected cells, but also in native tissues in vivo and even through the resolution of crystallized receptor structures [12]. In spite of these evidence and of the undisputed role of dimerization for Class C GPCRs [13, 14], the significance of dimerization remains controversial for the other classes of GPCRs [15] [16].

Thromboxane A_2 (TxA_2), a product of the oxidative metabolism of arachidonic acid, is a potent mediator of inflammation, a stimulator of platelet activation and aggregation, and a constrictor and mediator of proliferation of vascular and airway smooth muscle cells [17, 18]. In humans, the TP receptor is coded from a single gene that undergoes alternative splicing. This gives rise to two isoforms, termed TPα (343 residues) and TPβ (407 residues) which share identical N-terminal 328 amino acids and different C-terminal tails of 15 and 79 aminoacids, respectively [19]. The two isoforms primarily activate Gq/11 and G12/13 heterotrimeric G proteins, although coupling to Gs, Gi, and Gh has also been reported [19].

The TxA_2/TP receptor exerts a key role in the cardiovascular system by triggering thrombus formation [20]. This has been well demonstrated through the identification of a number of patients suffering from hemostatic defects with impaired TP receptor function due to single amino acid substitutions [21-24]. TP function appears to be tightly regulated, with suggestions that the deleterious cardiovascular effects of TPα could be limited by hetero-dimerization with either the TPβ [25, 26] or prostacyclin IP receptor [27, 28], which have been shown to regulate TPα trafficking and G protein coupling.

Different artificial systems, such as solubilization in detergents [5, 9, 29], purification and refolding in detergent/lipid mixed micelles [10], or incorporation into phospholipid bilayer [6, 7], have been used to isolate GPCR monomers thus allowing the characterization of

receptor monomer versus dimer pharmacology. Here, we directly compare in living cells the pharmacology and signaling of the homo-dimeric and monomeric forms of a Class A GPCR.

Recently, we have shown that TPα and TPβ homo-/hetero-dimers are characterized by contacts between hydrophobic residues in transmembrane domain 1 (TM1) of both protomers [26]. Indeed, TM1 and TM4/5 dimers, which appear more frequently in the crystals, are the most plausible dimeric models [30]. The disruption of this interface by alanine replacement of eight amino acids (Fig. 1) facing outward in dimerization-deficient mutants (DDMs) of one of the two TP isoforms is sufficient to drastically impair TPα-TPβ hetero-dimerization and to significantly interfere with agonist-induced TPα endocytosis. Here, we demonstrate that a panel of pharmacodynamically distinct agonists show reduced potencies, but similar efficacies in the activation of the DDM with respect to wild type (WT) TPα homo-dimer. In addition, these agonists maintained identical binding affinities for both DDM and WT receptors, suggesting a similar active receptor conformation.

Strikingly, we also show here that two single naturally occurring mutation in TM1, W29C and N42S, that either match or are in close proximity to two of the residues mutated in our DDM (W29 and L43, respectively), display a reduced potency to agonists accompanied by an impaired dimer formation both in ectopically transfected HEK-293T cells and, at least partially, in platelet membranes from patients. These naturally occurring mutations are associated in vitro with reduced TP receptor-stimulated platelet activation and in vivo bleeding disorders [23, 24]. Overall, these data suggest the impairment of TP dimerization as one possible molecular mechanism leading to reduced platelet aggregation and secretion in response to TP activators in vivo thereby affecting patients carrying these mutations.

2. MATERIALS AND METHODS

2.1 Reagents

Cell-culture media and supplements, animal serum, antibiotics, Lipofectamine® 2000, Opti-MEM I and molecular biology reagents were purchased from Invitrogen (Carlsbad, CA). Inositol-free Dulbecco's modified Eagle's medium (DMEM) was from ICN Pharmaceuticals Inc. (Costa Mesa, CA). Ultima Gold™ was from PerkinElmer Life and Analytical Sciences (Boston, MA), as were [5,6-^{3}H]SQ29,548 and myo-[2-^{3}H]inositol. U46619, I-BOP, 8-isoPGF$_{2\alpha}$ (8-iso Prostaglandin F$_{2\alpha}$), 8-isoPGE$_2$ (8-iso Prostaglandin E$_2$), PTA2, SQ29,548 and Ramatroban were from Cayman Chemical (Ann Arbor, MI). The Renilla Luciferase substrate for BRET^2, coelenterazine 400A was from Biotium (Hayward, CA). Anion exchange resin AG 1X-8 (formate form, 200–400 mesh) and Lowry dye-binding protein reagents were from Bio-Rad (Hercules, CA). All other reagents of the highest purity were available from Sigma-Aldrich (St. Louis, MO).

2.2 DNA constructs

The generation of human TPα receptor WT, DDM, and W29C DNA constructs was described elsewhere [23, 26, 31]. TPtrunc was obtained using the site direct mutagenesis kit (statagene) following manufacturer's instructions. Briefly TPtrunc was obtained by the insertion of a stop codon at the Ser57 of receptor sequence (Ser57-Stop) using specific primers carrying the Ser57-Stop mutation (FW: 5'-GCGCGGCAGGGTGGT**TAG**CACACGCGCTCCTCC-3'; RW: 5'-GGAGGAGCGCGTGTG**CTA**ACCACCCTGCCGCGC-3'). Mutated constructs were checked by Sanger analysis.

The cDNA encoding for the Gαq and Gβ1 was purchased from Missouri S&T cDNA Research Center (Rolla, MO, USA), while the cDNA encoding for GFP^{10}-$G\gamma_2$ and $G\alpha_q$-Rluc8 are as in Busnelli et al., [32] and have been previously characterized in Sauliere et al. [33]. Ultrapure plasmids for cell transfection were obtained using the QIAfilter Plasmid Kits (Qiagen, Hilden, Germany).

2.3 Cell culture and transient transfections

HEK293T host cells were purchased from the American Type Culture Collection (ATCC, Manassas, VA). Cells were routinely grown in Dulbecco's modified Eagle's medium (DMEM) supplemented with 10% FBS, 2 mM glutamine, 100 U/ml penicillin, 100 µg/ml streptomycin and 20 mM HEPES buffer pH 7.4, at 37°C in a humidified atmosphere of 95% air and 5% CO_2. For transfection, cells (5^{th}-20^{th} passage) were seeded onto tissue culture dishes previously coated with 5 µg/ml poly-D-lysine, and transfected at 30–40% confluence with an optimized 2:1 Lipofectamine 2000/DNA ratio as described previously [34]. All assays were performed 48 hours after transfection. In co-transfection experiments with TP and Gαq, plasmids were added in a 1:5 µg ratio, respectively.

2.4 Western immunoblotting

Transfected cells were lysed in lysis buffer containing a protease inhibitor cocktail (Sigma-Aldrich). Equal amounts of proteins were resolved on SDS-PAGE (10% acrylamide) and electro-transferred to Hybond-P membrane (GE Healthcare-Amersham, Piscataway, NJ). Blots were incubated overnight at 4°C in TBST [10mM Tris-HCl buffer, pH 8.0, 150 mM NaCl, 0.1% (v/v) Tween 20] containing 5% (w/v) skimmed milk. After washing with TBST, membranes were incubated at 25°C for 2 h with anti-Myc antibody diluted in TBST-milk

(Pierce, Rockford, IL). After washing in TBST, membranes were probed for 1.5 h at 25°C with horseradish peroxidase-conjugated goat anti-rabbit/mouse IgGs diluted in TBST-milk. Proteins were detected by chemiluminescence using the SuperSignal West Dura Extended Duration Substrate (Pierce) and visualized with Kodak Image Station 440 CF (Eastman Kodak Co., New Haven, CT). Band intensities were measured with the 'gel analyzer' ImageJ® plugin.

Platelets were probed using Abcam ab85544 a rabbit polyclonal antibody against the carboxyl-terminal of the human TP receptor as previously described [23].

2.5 Radioligand binding and total inositol phosphate assays

Ligand binding characteristics were determined on confluent adherent cells performing a mixed-type protocol [35] with the specific receptor antagonist [^{3}H]SQ29,548 (48 Ci/mmol) as previously described [31, 34, 36]. Briefly, heterologous competition studies involved concentrations of the indicated unlabeled ligands ranging from 0.1 nM to 30 μM and 1 nM of the labeled [^{3}H]SQ29,548. After 30 min incubation at 25°C, reactions were stopped by medium aspiration, and cells were washed with ice-cold PBS containing 0.2% (w/v) BSA and lysed in 0.5 N NaOH. Radioactivity was measured by liquid scintillation counting. Binding data were analyzed as described in Data and Statistical Analysis. Quantitation of the total labeled IP accumulation was performed using a conventional gravity flow column chromatography, as described previously [31, 34, 36]. Briefly, on day before assay, cells were labeled with 0.5 μCi [myo-2-^{3}H]inositol (17 Ci/mmol) for 18-20 hours in serum- and inositol-free DMEM containing 20 mM HEPES buffer, pH 7.4, and 0.5% (w/v) Albumax I. On day of assay, medium was replaced with serum-and inositol-free DMEM containing 25 mM LiCl and cells stimulated for 30 min with the indicated agonists. After medium removal, cells were lysed with 10 mM formic acid and lysates applied onto an anion exchange AG 1X-

8 column, formate form, 200-400 mesh. The total IP fraction was then eluted with 2 M ammonium formate/formic acid buffer at pH 5 and radioactivity determined by liquid scintillation counting.

2.6 Acceptor photobleaching Fluorescence Resonance Energy Transfer (FRET)

FRET measurements were performed with the laser-induced acceptor bleaching method previously reported [26, 37]. This type of analysis employing antibodies on living cells instead of fused fluorescent reporters to label the FRET pair offers the unique advantage over conventional FRET of only assaying surface receptors. Briefly, following in vivo exposure with anti-tag antibodies, cells were fixed in 4% (w/v) p-formaldehyde, and stained with Alexa Fluor 488- (donor fluorochrome) or 555 (acceptor fluorochrome)-conjugated secondary antibodies. Three images were captured before bleaching in the 488 and 555 nm channels using the line-by-line sequential mode without any averaging steps to reduce basal bleaching. Bleaching of the acceptor was performed within a region of interest (ROI) using 30 pulses of the 555 nm laser line at 100% intensity (each pulse 1.28 μsec/pixel). After bleaching seven images were acquired in the same channels to obtain a full curve for analysis. The number of bleaching steps was held constant throughout each experiment. FRET was quantified by measuring the average intensities of ROIs in the donor and acceptor fluorochrome channels before and after bleaching using the ImageJ software (http://rsbweb.nih.gov/ij/). To determine any change of fluorescence intensities not due to FRET occurring during the measurements, a distinct membrane 'sentinel' ROI of approximately the same size of the bleached ROI was measured in parallel, and all the results were normalized according to the background bleaching recorded in this sentinel ROI. Proper controls were performed to verify that no artifacts were generated in the emission spectra

throughout the experimental setup due to sample overheating. Forty measurements from four different transfections were performed for each experimental condition.

2.7 Bioluminescent Resonance Energy Transfer (BRET)

For BRET[2] experiments, HEK 293T cells were co-transfected with plasmids encoding for the GFP[10]-Gγ_2, Gβ_1, Gα_q-Rluc8 and WT or mutant TPα receptors. Forty-eight hours after transfection, cells were washed and detached with PBS, and resuspended in PBS+0.1% (w/v) glucose at room temperature. Cells were then distributed (80 µg of proteins per well) into a 96-well microplate (Wallac, Perkin Elmer, Monza, Italy) and incubated in the presence or absence of increasing concentrations of U46619 for 2 min before the addition of Coelenterazine 400A used at the final concentration of 5µM. BRET signal between Rluc8 and GFP[10] was measured immediately in the microplate reader (Infinite F500, Tecan, Grödig, Austria). The BRET signal was calculated as the ratio of the light emitted by GFP[10] (510–540 nm) over the light emitted by Rluc8 (370–450 nm). The changes in BRET induced by the ligands were expressed as "BRET ligand effect", obtained by subtracting the BRET signal detected in the presence of PBS by the BRET signal detected in the presence of the specific concentration of the U46619.

2.8 Data and statistical analysis

All results are presented as means ± S.E. When indicated, ANOVA followed by post-hoc test for multiple comparisons was performed. Data from radioligand binding were evaluated by a nonlinear, least-squares curve-fitting procedure using GraphPad Prism version 5, implemented with the n-ligand m-binding site model, as described in the LIGAND computer program [38]. Concentration-response curves were evaluated using Prism 5, that uses the

four-parameter logistic model as described in the ALLFIT program [39]. Parameter errors are all expressed as percentage coefficients of variation (%CV) and calculated by simultaneous analysis of at least three independent experiments performed in duplicate or triplicate. All parameter comparisons have been performed based on the F test for extra sum of square as implemented in GraphPad Prism. All curves shown are generated by computer fitting.

3. RESULTS

3.1 Antagonist Binding and Receptor Expression

To allow a proper comparison of receptor responses, transfection conditions were adjusted to ensure comparable levels of ectopic expression of WT and DDM (I25A, W29A, C35A, V36A, L39A, L43A, L44A, S47A mutant) of human TPα receptors in HEK293T cells in a range between 0.8-1.3 pmol/mg protein (Table 1). As expected, mock transfected cells showed no detectable binding to [^{3}H]-SQ29,548 (data not shown), whereas analysis of binding curves of cells transiently transfected with WT TPα displayed a monophasic behavior corresponding to a single-site model by computer modeling (Fig. 2A), with binding parameters as previously reported [31, 34, 36]. Of notice, the TPα DDM displayed a binding affinity not statistically different from the corresponding WT receptor (Table 1). These results strongly indicate that DDM, is trafficked to the cell surface (Fig. 2B), can be expressed at physiological relevant levels [40] and exhibits an overall conformation and folding not significantly different from that of WT.

3.2 Effect of TM1 mutations on homo-dimerization of TPα receptor

We previously reported that WT TPα and TPβ form hetero-dimers through contacts between hydrophobic residues of TM1 with mutations in the TM1 stretch impairing TPα-TPβ association regardless of which TP member of the co-transfected pair contains the mutated residues [26]. To confirm that the TPα DDM is impaired also in homo-dimer formation, we co-expressed WT and DDM mutant TPα tagged with an N-terminal myc epitope in HEK293T cells. Western blotting revealed distinct bands migrating on SDS-PAGE at the relative molecular masses (*M*r) predicted [25] for monomeric and dimeric receptors for WT transfectants (Fig. 3A). Interestingly, unlike the WT most of the DDM exists as a monomer. There was a significant reduction of the density of the dimeric band in DDM accompanied by increased intensity of monomeric bands referred to as glycosylated and non-glycosylated TP monomers as previously reported [25] ($p < 0.001$, Fig. 3B).

To obtain direct evidence that mutations in the TM1 interface of DDM impair TPα dimerization, we performed FRET analysis using the laser-induced acceptor photobleaching method [37]. In this type of analysis fluorescence emission by a donor fluorochrome is quenched due to direct transfer of excitation energy to an acceptor fluorochrome. Upon laser-induced acceptor bleaching, this FRET is blunted and the donor signal is de-quenched. Accordingly, HEK293T cells co-transfected with different TPα pairs, tagged with HA and c-myc epitopes, were in vivo labeled with their corresponding anti-tag antibodies, fixed, subjected to indirect immunofluorescence and then imaged by laser scanning confocal microscopy. Figure 3C demonstrates our approach. Note that an increase of fluorescence signal emitted by the donor fluorochrome resulting from de-quenching (i.e. FRET efficiency) is only present in analyzed cells co-expressing the WT TPα pair (Fig. 3D), suggesting that only in these cells energy transfer is possible and thus dimer formation occurs. On the contrary, no increase in signal emitted by the donor fluorochrome is present in the DDM

expressing cells, suggesting that mutations in TM1 are sufficient to prevent energy transfer from donor to acceptor, and thus to impair homo-dimerization of TPα.

To further characterize this phenomenon we repeated the experiments by transfecting cells with different levels of the TPα DNA (500, 5 and 0.5 ng) (Fig. 3D). Even at the highest levels of DDM receptor expression we could still not detect any interaction between receptor monomers although we could clearly visualize both tagged versions of the receptor at the cell surface (Fig. 2B). These results suggest that homo-dimerization of TPα within a large range of expression levels, including physiological ones (corresponding to the intermediate level [40], is strongly destabilized in the receptor bearing TM1 mutations.

3.3 Basal Activity of DDM receptor in the presence of overexpression of Gαq

A key feature of the TP receptor is a lack of constitutive activity (CA), even following increased expression of receptor, Gαq, or a combination of both [31, 36]. To further assess the pharmacological characteristics of the DDM receptor, its basal activity was compared with that of the WT by assaying total IP production in the absence of agonist stimulation (Fig. 4). These experiments were also repeated in the presence of Gαq overexpression to try and promote CA at these receptors. In the mock condition, a 5-fold overexpression of Gαq induced an increase of total IP production (about 50% compared to no Gαq, Fig. 4), likely due to a general increase in this G protein as previously reported [36]. Co-expression of either the WT or DDM failed to further enhance total IP production. These results demonstrate that the DDM, like the WT and other TP receptor mutants tested thus far, does not show any appreciable CA [31, 34, 36].

3.4 Pharmacological characterization of the DDM functional activity

To fully characterize DDM activity, IP accumulation was evaluated in HEK293T cells transiently expressing WT or DDM in response to a series of pharmacodynamically different TP agonists, including the full agonists U46619 and I-BOP and the partial agonists 8-iso-$PGF_{2\alpha}$ and 8-isoPGE_2 (Fig. 5A, B). Computer-assisted analysis of concentration-response curves showed that EC_{50} values for the different agonists at DDM were significantly shifted rightward as compared to WT ($p < 0.01$; Table 2). 8-iso-$PGF_{2\alpha}$ and 8-isoPGE_2 activated the DDM and the WT with equal efficacies, in accordance with their pharmacodynamic profiles as partial agonists (Fig. 5A, B).

We also assessed the ability of the TP receptor antagonist SQ29,548 and the structurally unrelated TP and DP_2 antagonist ramatroban, to inhibit agonist (U46619, 1 μM)-induced IP production by WT and DDM receptors (Fig. 5C, D). Both antagonist inhibition curves at the DDM were significantly ($p < 0.01$) leftward shifted with IC_{50} values around 5-6 fold lower than the WT (WT: IC_{50} = 254 nM ± 66 %CV and 144 ± 29 %CV for SQ29,548 and ramatroban, respectively; DDM: 45 nM ± 61 %CV and 29 ± 56 %CV for SQ29,548 and ramatroban, respectively). This apparent increase in antagonist potencies is likely a consequence the reduced potency of U46619 to activate DDM. Collectively, these data indicate that the DDM form of TPα less efficiently responds to agonist activation across a panel of compounds endowed with different intrinsic activities than the WT homo-dimeric form.

To confirm that the pharmacological profile of our artificial DDM is not due exclusively to the presence of the eight mutations in TM1, we co-transfected the WT TP receptor with a truncated form of TP coding only for the N terminal and TM1 regions (TPtrunc), an approach previously shown to destabilize the quaternary structure and the interaction interfaces of rhodopsin [41]. While TPtrunc alone was pharmacologically silent, co-transfection with the

WT TP receptor reduced receptor function (Fig. 6A). Careful analysis of dose-response curves revealed that WT TP receptor plus TPtrunc produced a receptor profile similar to DDM with potencies (EC_{50} = 84.8 nM ± 50 %CV and 111 nM ± 72 %CV, respectively) and efficacies not statistically different. Notably, TPtrunc is expressed at cellular surface and laser-induced acceptor bleaching FRET demonstrated that it is able to dimerize with WT TP receptor (Fig. 6B). Thus, we can assume that the presence of an excess (1:10) of TPtrunc interfere with the WT-WT TP dimer formation, forcing WT TP receptor into a monomeric form. This, in turn, suggests that the pharmacological profile observed for the DDM might indeed be due to its monomeric state and not to merely the presence of mutations. It is likely that TPtrunc interferes with the quaternary structure of the homo-dimer, but do not necessarily block dimerization completely.

Transfection of a mutated form of the TPtrunc (carrying the same eight mutations as the DDM, TPtrunc TM1) with the WT TP receptor (Fig. 6A) resulted in concentration response curve identical to that of WT TP alone (EC_{50} = 23.2 nM ± 27 %CV and 35.6 nM ± 31 %CV, respectively) demonstrating the specificity of the functional interference exerted by the truncated form of the receptor on TP dimers/oligomers and the importance of these eight amino acids in TM1 to WT TP receptor interaction.

3.5 Ligand binding profile of the DDM receptor

The ligand binding capacities of the WT and DDM receptors transiently expressed in HEK-293T cells were also tested to assess whether the ligand binding pocket and/or the active receptor conformation was affected by mutations. Heterologous competition curves performed with [^{3}H]-SQ29,548 and several unlabeled agonists revealed unchanged affinities between both WT and DDM receptor constructs and an entire panel of compounds, including the two partial agonists 8-iso-$PGF_{2\alpha}$ and 8-isoPGE_2 (Fig. 7A, B and Table 3). In addition to

SQ29,548 (Table 1), also the structurally unrelated TP antagonist, PTA2 (Fig. 7C and D) did not show any difference in binding affinities between receptors (K_i = 3.6 μM ± 68 %CV and K_i = 2.4 μM ± 67 %CV for WT and DDM, respectively). These data, therefore, are consistent with similar agonist-induced receptor conformations and G protein coupling for both WT and DDM, suggesting that the difference in signaling efficiency might be due to a difference in G protein activation, rather than to a difference in receptor conformational states.

3.6 Impact of W29C and N42S mutations on dimerization and pharmacology of TPα receptor

3.6.1 Impact in human platelets

As mentioned above a patient heterozygous for the TP receptor variant W29C with impaired platelet response to TP receptor agonists has been previously identified [23]. In this study in HEK293T U46619 was demonstrated to be less potent at the W29C variant versus WT in inducing a rise of cytosolic free Ca^{2+}, although the molecular mechanisms underlying this difference were not fully elucidated [23]. Importantly W29 is one of the eight residues mutated in our DDM [26] (Fig. 1). In order to study the impact of the single W29C mutation on dimerization of TP receptor, the endogenously expressed receptor in platelets was detected with an antibody directed against the carboxyl-terminal of human TPα receptor. The TP receptor can be found in monomeric, dimeric and higher oligomeric forms in human platelets from healthy donors (Fig. 8A, HD) [25]. Platelets from the W29C patient show only a modest reduction of the dimeric TP form (Fig. 8A, W29C), although quantification over multiple experiments seems to suggest a decrease of both dimeric and oligomeric forms of receptor (Fig. 8B) that, however, did not reach statistical significance. These results were not totally

unexpected, considering that the patient is heterozygous for the W29C mutation [23], and therefore is still able to express a substantial amount of dimeric WT TP.

3.6.2 Impact in transfected HEK293T

To further investigate the functional significance of the W29C mutation, we again used laser-induced acceptor bleaching FRET methodology outlined above on transfected HEK 293T cells. Intriguingly, there was no recovery of donor fluorescence due to a lack of energy transfer in cells overexpressing the WT-W29C pair (103% ± 0.8 SE, Fig. 9A and B), suggesting minimal proximity and hence less dimerization between donor/acceptor proteins. Similar data were also obtained when we tested another naturally occurring mutation, N42S [24] with minimal evident energy transfer in our FRET studies (Fig 9B). It should be noted that this residue is just one position upstream of the L43 and L44 residues mutated in our DDM (Fig. 1). Indeed, we do not have a crystal structure of our receptor, but only an homology model [26], and thus this slight difference might be explained by a possible dissimilarity between our model and the real TP structure. Collectively, these results strongly suggest that TPα dimerization is impaired with W29C or the N42S receptor variant, in striking agreement with the behavior of our artificial DDM.

3.6.3 Impact on pharmacology

We therefore further investigated the pharmacological profile of the W29C natural variant in functional assays (Fig. 10). Concentration-response curves of all agonists for W29C were significantly shifted rightward as compared to WT, with calculated potencies (EC_{50} = 150 nM ± 21 %CV and 75 ± 9 %CV for U46619 and I-BOP, Panel A; EC_{50} = 1896 nM ± 37 %CV and 43280 ± 56 %CV for 8-iso-PGE_2 and 8-iso$PGF_{2\alpha}$, Panel B) consistent with those of the artificial DDM (Table 2). Interestingly, the pharmacological profile of the naturally occurring

W29C mutant exactly matches that of the artificial DDM. Additionally, 8-iso-$PGF_{2\alpha}$ and 8-isoPGE_2 also confirmed their pharmacodynamic profile as partial agonists activating the W29C variant with equal efficacies (Emax = 3.2 ± 5 %CV and 3.6 ± 16 %CV, respectively). The antagonists SQ29,548 and ramatroban specifically inhibited U46619-induced total IP production by W29C with results not statistically different from DDM (data not shown).

3.7 Direct G protein activation

To further support our hypothesis that the differences in signaling efficiencies might be due to a difference in G protein activation and not a difference in receptor conformational states, we performed a direct measure of G protein activation using an intramolecular $BRET^2$-based biosensor [42]. In this assay Renilla luciferase 8 (Rluc8), used as energy donor, is located on the Gαq subunit, while GFP^{10}, the energy acceptor, is located on the Gγ subunit of the G protein. Thus, a decrease of the BRET signal triggered by agonist-induced receptor activation is indicative of an opening of the Gα-Gβγ interface, reflecting the initial event of Gq protein activation [32, 43]. Thus, after setting the optimal transfection conditions to assure the same level of basal BRET signal for WT and different TPα mutants [32, 36], concentration-response curves of the stable agonist U46619 have been performed in HEK293T cells expressing equal amount of WT and mutant TPα receptors. As it is clear from Figure 11A, the U46619 curve obtained with the DDM mutant shows a significant ($p < 0.01$) decrease in potency with more than a five fold rightward shift with respect to the curves obtained with the WT TPα receptor (Table 4). Similar results were obtained with the N42S and W29C variants (Fig. 11B). Comparison of EC_{50} for WT and W29C reveals a perfect agreement with those obtained from the analysis of total IP dose-response curves (see Table 2 and Fig. 10A). Statistical comparison of potencies provided a significant difference between parameters

obtained with WT and the different TPα variants, thus demonstrating a reduced "efficiency" in G protein activation by the mutated proteins (Table 4).

4. DISCUSSION

Despite the intense effort devoted to demonstrate the mechanism(s) by which GPCRs form complexes with each other, the physiological relevance of this phenomenon still remains elusive [11, 15] [16]. Hetero-dimerization has been shown to be an absolute requirement for the activity of some Class C GPCRs [13, 14] and the cell-surface delivery of other GPCRs [44, 45]. The process can also be regarded as a way of creating a receptor complex endowed with unique signaling features in response to the binding of specific ligands [46, 47]. A more difficult issue to characterize is the role of receptor homo-dimerization in terms of receptor activation and function. In order to address this question we characterized the pharmacological activity of the human TP receptor, containing either artificial (DDM TP) [26] or naturally occurring (W29C and N42S) [23, 24] mutations in TM1, impaired in its ability to spontaneously form receptor dimers.

The main key finding of the present study comes from the detailed pharmacological characterization of the DDM TP receptor using a combination of antagonists and full and partial agonists in living cells. Unlike the WT receptor, which spontaneously forms homo-dimers at physiological expression levels, DDM, which is significantly impaired in its ability to form dimers, displays a significant reduction in agonist potency in comparison to the WT. Despite a reduction in agonist potency, the WT and DDM receptors have indistinguishable overall and active conformations as assessed by antagonist and agonist ligand-binding studies and possess similar abilities to bind and induce G_q-mediated signaling. However, the DDM receptor clearly shows a reduced 'efficiency' in G protein activation. Thus, TM1 appears to

be an important region contributing to the normal function of the TPα receptor in vitro. To support these findings two recent studies examining naturally occurring variants in the TPα receptor, W29C and N42S identified in two patients with bleeding disorders, demonstrated that platelets from these patients exhibited a decrease in TP receptor-stimulated activation. We now demonstrate that both W29C and N42S TPα receptor variants are impaired in their ability to dimerize in a recombinant system, and with a partial reduction also apparent in platelets from these patients. Strikingly, one of these naturally occurring mutations (W29C) exactly matches, and the other (N42S) is just one residue upstream of two out of the eight residues mutated in our artificial DDM. Thus, we suggest that a single mutation in TM1 might be sufficient to impair homo-dimer formation, and may in part be responsible for the observed decrease in TP receptor functionality observed in vivo.

Although DDM is expressed at the cell surface at physiologically relevant levels it is drastically impaired in its tendency to form homo-dimers over a range of different expression levels, as demonstrated by western blotting and acceptor photobleaching FRET analysis. Ligand-binding studies with the TP receptor antagonist SQ29,548 confirm normal protein folding, and suggest a conserved overall protein conformation, as also previously postulated by molecular dynamic simulations [26].

In functional assays DDM signaling was significantly impaired versus WT with a significant rightward shift in agonist-potency across a panel of full and partial TP receptor agonists. In agreement with this loss of agonist activity, two structurally different antagonists demonstrated an apparent increase in their potency. Most importantly, despite their reduced potency in promoting DDM activation, all the ligands investigated retained their respective pharmacological profiles as either full or partial agonists. In addition, the basal activity of DDM is similar to that of WT and not affected by increased expression of its cognate G protein, a further validation of TP 'resistance' to CA [31, 34, 36].

Importantly, co-transfection of the WT TP receptor with a truncated form of TP coding only for the N terminal and TM1 regions produced a pharmacological profile similar to that of the DDM. Because TPtrunc is able to dimerize with WT receptor, its co-expression very likely impairs WT-WT TP dimer formation, forcing TP receptor into a monomeric form. This, in turn, suggests that the monomeric form of TP, as for many other GPCRs, is able to signal, and that the pharmacological profile observed for the DDM might indeed be due to its monomeric state and not to merely the presence of mutations.

In addition, the phenotype described for this 'artificial' DDM matches the phenotypes of the W29C and N42S TPα natural variants [23, 24]. In these studies we suggested that reduced TP receptor surface expression seen in the W29C patient reduced TP receptor-stimulated platelet aggregation. We now speculate that in addition to this reduction in surface expression, since both the W29C and N42S are impaired in the dimerization with WT, the heterozygous patients may also display a shift in the normal equilibrium from TPα homo-dimers to monomers with a consequent overall decrease in agonist potency. Western blotting of patient platelets TPα reveals receptor in monomeric, dimeric, and higher-order oligomeric forms in agreement with previously published results [25]. These blots suggested that there maybe a modest reduction in TPα oligomer although it should be noted that both patients are heterozygous for each variant and therefore will also express WT TP receptor. The presence of WT TP receptor is likely to mask our ability to see a statistically significant reduction in dimer formation. Intriguingly, each of these variants shows comparable levels of maximal receptor responsiveness to agonists when compared to WT, but have reduced potency in second messenger production [23, 24], as it is the case for the artificial DDM. It is therefore tempting to speculate that the impairment in dimer formation might represent a crucial molecular mechanism of the decreased platelet response to TP agonists in vivo.

In an attempt to clarify whether the change in agonist potency might arise from a change in the ligand-binding pocket and/or in an allosteric effect within the protomers of the TPα homo-dimer [48], we analyzed the agonist binding profile of a series of compounds endowed with different intrinsic activities. All the tested agonists displayed equal binding affinities for the DDM and WT receptors, thus indicating that the agonist-induced active state of the monomeric and dimeric proteins are similar, and supporting the absence of any allosteric modulation across protomers of the TPα homo-dimer at the level of the binding pocket. Notably, the DDM retains high affinity agonist binding that is indicative of a normal coupling with the cognate G proteins. Thus, differences able to explain a reduced potency of agonists in DDM activation must be sought downstream of the TP receptor itself, likely at the G protein level. Indeed, direct analysis of G protein activation by a $BRET^2$-based technique clearly demonstrates a reduced efficiency in G protein activation for our artificial DDM as well as for the N42S and, especially, W29C variants.

Collectively, all these observations strongly support the notion that reduced agonist potencies demonstrated by the DDM in second messenger production do not arise from a change in the receptor state, i.e. by a variation in agonist-induced conformation, or in the receptor ability to recognize pharmacodynamically different agonists, or in its ability to interact with G proteins. Rather, these data are suggestive of a reduced signaling strength, due to a reduced efficiency in G protein activation.

While we recognize that we cannot completely rule out the possibility that the differences observed in our DDM might depend upon the presence of the mutations alone, the fact that a single mutation (W29C or N42S) or dimerization with a truncated and silent form of the receptor closely match the pharmacology of our DDM, convincingly indicates that the particular pharmacological profile observed with our TP mutants may be the result of an impairment of dimer/oligomer formation.

In respect to this, contrasting data are emerging on G protein activation by different dimeric GPCRs. Some data support a model of a higher efficiency of G protein activation in dimers/oligomers [29, 49, 50], whilst others demonstrate a similar degree of activation [6, 7], or even a reduced G protein coupling efficiency by dimeric ensembles [9, 10]. While it is possible that different receptors might simply behave differently from another, it is also true that the same receptor seems to behave differently in different experimental conditions as shown with rhodopsin isolated by filtration techniques [29] versus expression in a phospholipid bilayer [7]. To our knowledge, our functional results are the first to be obtained with a dimeric and a monomeric form of a Class A GPCR expressed in living cells that is not artificially purified/reconstituted. More data on other receptor systems will certainly come in the near future to clarify this issue, as it has been recently the case for the glucagon-like peptide-1 receptor, where homo-dimer formation seems important for the control of signal bias [51].

Finally, while the stoichiometry of the receptor-G protein unit still remains an open question, a number of studies favor a 2:1 stoichiometry, corroborating the hetero-pentameric structure of two protomers binding one heterotrimeric G protein [50, 52-55]. A number of biochemical studies suggest the involvement of several distinct G protein regions in receptor interaction [56], both on the α [57, 58], as well as on the γ-subunit [59, 60]. While the C-terminal sites on the α-subunit have been confirmed by crystallization to interact with opsin/metarhodopsin [61] and β_2-AR [62], unexpectedly, no direct interaction between β_2-AR and Gβ- or Gγ-subunits have been detected [62]. Indeed biochemical studies suggest that β_2-AR exists as a dimer in living cells [63] and that the C-terminal of Gα and of Gγ are further apart in the G protein heterotrimer than the width of a monomeric GPCR [64]. Thus, the 2:1 stoichiometry is consistent with multiple contact sites of the G protein with two different protomers [65, 66], whereas the heterotrimer appears necessary for efficient

coupling to a GPCR [67]. In light of our data and of this 'double docking' model described above we can speculate that, when a secondary site of contact is available due to the presence of a homo-dimer, a stronger coupling with the cognate G protein is favored, hence more efficient signaling is then possible. Indeed, the presence of transducin has been shown to stabilize the dimeric conformation of rhodopsin, while the presence of synthetic peptides that disrupt rhodopsin dimerization, similar to our truncated TP receptor construct, inhibited such stabilization [41].

In conclusion, our data propose that TPα receptor dimer formation favors a more efficient signaling complex, increasing agonist potency. This augmented ability is very likely the result of a more efficient G protein activation. Given that TP monomers and homo-dimers are, presumably, in equilibrium at steady state [68, 69], it is possible that when a single TPα protomer makes a complex with a TPβ [25, 26] or IP protomer [27] there would be a shift in the equilibrium from TPα homo-dimers to monomers with a consequent overall decrease in agonist potency, which may be important in thrombosis-related diseases. In this respect, the impairment of W29C and N42S to form dimers with WT receptor may represent one molecular mechanism through which platelet TP receptor dysfunction affects the patient(s) carrying these mutations.

Acknowledgements

The authors would like to acknowledge Prof. Francesca Fanelli for drawing of Figure 1.

This work was supported in part by a grant from Regione Lombardia (SAL-02) and from Fondazione Banca del Monte di Lombardia (to G.E.R.) - MB is a Post-doctoral Research Fellow of the Umberto Veronesi Foundation. SJM is a Senior Research Fellow of the British Heart Foundation.

Conflict of interest Statement: None declared

5. REFERENCE

[1] R.J. Lefkowitz, Seven transmembrane receptors: something old, something new, Acta Physiol (Oxf) 190(1) (2007) 9-19.

[2] R. Fredriksson, M.C. Lagerstrom, L.G. Lundin, H.B. Schioth, The G-protein-coupled receptors in the human genome form five main families. Phylogenetic analysis, paralogon groups, and fingerprints, Mol Pharmacol 63(6) (2003) 1256-72.

[3] C.B. Brink, B.H. Harvey, J. Bodenstein, D.P. Venter, D.W. Oliver, Recent advances in drug action and therapeutics: relevance of novel concepts in G-protein-coupled receptor and signal transduction pharmacology, Br J Clin Pharmacol 57(4) (2004) 373-87.

[4] C.H. Heldin, Dimerization of cell surface receptors in signal transduction, Cell 80(2) (1995) 213-23.

[5] O.P. Ernst, V. Gramse, M. Kolbe, K.P. Hofmann, M. Heck, Monomeric G protein-coupled receptor rhodopsin in solution activates its G protein transducin at the diffusion limit, Proc Natl Acad Sci U S A 104(26) (2007) 10859-64.

[6] T.H. Bayburt, A.J. Leitz, G. Xie, D.D. Oprian, S.G. Sligar, Transducin activation by nanoscale lipid bilayers containing one and two rhodopsins, J Biol Chem 282(20) (2007) 14875-81.

[7] M.R. Whorton, B. Jastrzebska, P.S. Park, D. Fotiadis, A. Engel, K. Palczewski, R.K. Sunahara, Efficient coupling of transducin to monomeric rhodopsin in a phospholipid bilayer, J Biol Chem 283(7) (2008) 4387-94.

[8] M.R. Whorton, M.P. Bokoch, S.G. Rasmussen, B. Huang, R.N. Zare, B. Kobilka, R.K. Sunahara, A monomeric G protein-coupled receptor isolated in a high-density lipoprotein particle efficiently activates its G protein, Proc Natl Acad Sci U S A 104(18) (2007) 7682-7.

[9] J.F. White, J. Grodnitzky, J.M. Louis, L.B. Trinh, J. Shiloach, J. Gutierrez, J.K. Northup, R. Grisshammer, Dimerization of the class A G protein-coupled neurotensin receptor NTS1 alters G protein interaction, Proc Natl Acad Sci U S A 104(29) (2007) 12199-204.

[10] L. Arcemisbehere, T. Sen, L. Boudier, M.N. Balestre, G. Gaibelet, E. Detouillon, H. Orcel, C. Mendre, R. Rahmeh, S. Granier, C. Vives, F. Fieschi, M. Damian, T. Durroux, J.L. Baneres, B. Mouillac, Leukotriene BLT2 receptor monomers activate the G(i2) GTP-binding protein more efficiently than dimers, J Biol Chem 285(9) (2010) 6337-47.

[11] S. Ferre, V. Casado, L.A. Devi, M. Filizola, R. Jockers, M.J. Lohse, G. Milligan, J.P. Pin, X. Guitart, G protein-coupled receptor oligomerization revisited: functional and pharmacological perspectives, Pharmacol Rev 66(2) (2014) 413-34.

[12] V. Katritch, V. Cherezov, R.C. Stevens, Structure-function of the G protein-coupled receptor superfamily, Annu Rev Pharmacol Toxicol 53 (2013) 531-56.

[13] J.H. White, A. Wise, M.J. Main, A. Green, N.J. Fraser, G.H. Disney, A.A. Barnes, P. Emson, S.M. Foord, F.H. Marshall, Heterodimerization is required for the formation of a functional GABA(B) receptor, Nature 396(6712) (1998) 679-82.

[14] J. Kniazeff, L. Prezeau, P. Rondard, J.P. Pin, C. Goudet, Dimers and beyond: The functional puzzles of class C GPCRs, Pharmacol Ther 130(1) (2011) 9-25.

[15] G. Milligan, The Prevalence, Maintenance and Relevance of GPCR Oligomerization, Mol Pharmacol (2013).

[16] N.A. Lambert, J.A. Javitch, CrossTalk opposing view: Weighing the evidence for class A GPCR dimers, the jury is still out, J Physiol 592(Pt 12) (2014) 2443-5.

[17] S. Narumiya, Y. Sugimoto, F. Ushikubi, Prostanoid receptors: structures, properties, and functions., Physiological Reviews 79(4) (1999) 1193-226.

[18] A.N. Hata, R.M. Breyer, Pharmacology and signaling of prostaglandin receptors: multiple roles in inflammation and immune modulation, Pharmacol Ther 103(2) (2004) 147-66.

[19] D.F. Woodward, R.L. Jones, S. Narumiya, International Union of Basic and Clinical Pharmacology. LXXXIII: Classification of Prostanoid Receptors, Updating 15 Years of Progress, Pharmacol Rev (2011).

[20] V. Capra, M. Back, S.S. Barbieri, M. Camera, E. Tremoli, G.E. Rovati, Eicosanoids and their drugs in cardiovascular diseases: focus on atherosclerosis and stroke, Med Res Rev 33(2) (2013) 364-438.

[21] T. Hirata, A. Kakizuka, F. Ushikubi, I. Fuse, M. Okuma, S. Narumiya, Arg60 to Leu mutation of the human thromboxane A2 receptor in a dominantly inherited bleeding disorder, Journal of Clinical Investigation 94(4) (1994) 1662-7.

[22] A.D. Mumford, B.B. Dawood, M.E. Daly, S.L. Murden, M.D. Williams, M.B. Protty, J.C. Spalton, M. Wheatley, S.J. Mundell, S.P. Watson, A novel thromboxane A2 receptor D304N variant that abrogates ligand binding in a patient with a bleeding diathesis, Blood 115(2) (2010) 363-9.

[23] A. Mumford, S. Nisar, L. Darnige, M. Jones, C. Bachelot-Loza, S. Gandrille, F. Zinzindoue, A.M. Fischer, S. Mundell, P. Gaussem, Platelet dysfunction associated with the novel Trp29Cys thromboxane A(2) receptor variant, J Thromb Haemost 11(3) (2012) 547-54.

[24] S.P. Nisar, M. Lordkipanidze, M.L. Jones, B. Dawood, S. Murden, M.R. Cunningham, A.D. Mumford, J.T. Wilde, S.P. Watson, S.J. Mundell, G.C. Lowe, U.K.G.s.g. on behalf of the, A novel thromboxane A2 receptor N42S variant results in reduced surface expression and platelet dysfunction, Thromb Haemost 111(5) (2014) [Epub ahead of print].

[25] G. Laroche, M.C. Lepine, C. Theriault, P. Giguere, V. Giguere, M.A. Gallant, A. de Brum-Fernandes, J.L. Parent, Oligomerization of the alpha and beta isoforms of the thromboxane A2 receptor: relevance to receptor signaling and endocytosis, Cell Signal 17(11) (2005) 1373-83.

[26] F. Fanelli, M. Mauri, V. Capra, F. Raimondi, F. Guzzi, M. Ambrosio, G.E. Rovati, M. Parenti, Light on the structure of thromboxane A(2) receptor heterodimers, Cell Mol Life Sci 68(18) (2011) 3109-3120.

[27] S.J. Wilson, A.M. Roche, E. Kostetskaia, E.M. Smyth, Dimerization of the human receptors for prostacyclin and thromboxane facilitates thromboxane receptor-mediated cAMP generation, J Biol Chem 279(51) (2004) 53036-47.

[28] S.J. Wilson, J.K. Dowling, L. Zhao, E. Carnish, E.M. Smyth, Regulation of thromboxane receptor trafficking through the prostacyclin receptor in vascular smooth muscle cells: role of receptor heterodimerization, Arterioscler Thromb Vasc Biol 27(2) (2007) 290-6.

[29] B. Jastrzebska, D. Fotiadis, G.F. Jang, R.E. Stenkamp, A. Engel, K. Palczewski, Functional and structural characterization of rhodopsin oligomers, J Biol Chem 281(17) (2006) 11917-22.

[30] A. Cordomi, G. Navarro, M.S. Aymerich, R. Franco, Structures for G-Protein-Coupled Receptor Tetramers in Complex with G Proteins, Trends Biochem Sci 40(10) (2015) 548-51.

[31] V. Capra, A. Veltri, C. Foglia, L. Crimaldi, A. Habib, M. Parenti, G.E. Rovati, Mutational analysis of the highly conserved ERY motif of the thromboxane A2 receptor: alternative role in G protein-coupled receptor signaling, Mol Pharmacol 66(4) (2004) 880-9.

[32] M. Busnelli, G. Kleinau, M. Muttenthaler, S. Stoev, M. Manning, L. Bibic, L.A. Howell, P.J. McCormick, S. Di Lascio, D. Braida, M. Sala, G.E. Rovati, T. Bellini, B. Chini, Design

and Characterization of Superpotent Bivalent Ligands Targeting Oxytocin Receptor Dimers via a Channel-Like Structure, J Med Chem 59(15) (2016) 7152-66.

[33] A. Sauliere, M. Bellot, H. Paris, C. Denis, F. Finana, J.T. Hansen, M.F. Altie, M.H. Seguelas, A. Pathak, J.L. Hansen, J.M. Senard, C. Gales, Deciphering biased-agonism complexity reveals a new active AT1 receptor entity, Nat Chem Biol 8(7) (2012) 622-30.

[34] M. Ambrosio, F. Fanelli, S. Brocchetti, F. Raimondi, M. Mauri, G.E. Rovati, V. Capra, Superactive mutants of thromboxane prostanoid receptor: functional and computational analysis of an active form alternative to constitutively active mutants, Cell Mol Life Sci 67(17) (2010) 2979-89.

[35] G.E. Rovati, Ligand-binding studies: old beliefs and new strategies, Trends Pharmacol Sci 19(9) (1998) 365-9.

[36] V. Capra, M. Busnelli, A. Perenna, M. Ambrosio, M.R. Accomazzo, C. Gales, B. Chini, G.E. Rovati, Full and partial agonists of thromboxane prostanoid receptor unveil fine tuning of receptor superactive conformation and G protein activation, PloS one 8(3) (2013) e60475.

[37] P. Konig, G. Krasteva, C. Tag, I.R. Konig, C. Arens, W. Kummer, FRET-CLSM and double-labeling indirect immunofluorescence to detect close association of proteins in tissue sections, Lab Invest 86(8) (2006) 853-64.

[38] P.J. Munson, D. Rodbard, LIGAND: A Versatile Computerized Approach for Characterization of Ligand-Binding Systems, Anal. Biochem. 107 (1980) 220-239.

[39] A. De Lean, P.J. Munson, D. Rodbard, Simultaneous analysis of families of sigmoidal curves: application to bioassay, radioligand assay, and physiological dose-response curves, Am. J. Physiol. 235 (1978) E97-E102.

[40] A. Hedberg, S.E. Hall, M.L. Ogletree, D.N. Harris, E.C.-K. Liu, Characterization of [5,6-3H]SQ 29,548 as a high affinity radioligand, binding to thromboxane A2/prostaglandin

H2 receptor in human platelets, Journal of Pharmacology and Experimental Therapeutics 245 (1988) 786-792.

[41] B. Jastrzebska, Y. Chen, T. Orban, H. Jin, L. Hofmann, K. Palczewski, Disruption of Rhodopsin Dimerization with Synthetic Peptides Targeting an Interaction Interface, J Biol Chem 290(42) (2015) 25728-44.

[42] M.A. Ayoub, Resonance Energy Transfer-Based Approaches to Study GPCRs, Methods Cell Biol 132 (2016) 255-92.

[43] C. Gales, J.J. Van Durm, S. Schaak, S. Pontier, Y. Percherancier, M. Audet, H. Paris, M. Bouvier, Probing the activation-promoted structural rearrangements in preassembled receptor-G protein complexes, Nature structural & molecular biology 13(9) (2006) 778-86.

[44] S. Bulenger, S. Marullo, M. Bouvier, Emerging role of homo- and heterodimerization in G-protein-coupled receptor biosynthesis and maturation, Trends Pharmacol Sci 26(3) (2005) 131-7.

[45] G. Milligan, The role of dimerisation in the cellular trafficking of G-protein-coupled receptors, Curr Opin Pharmacol 10(1) (2010) 23-9.

[46] S.C. Prinster, C. Hague, R.A. Hall, Heterodimerization of g protein-coupled receptors: specificity and functional significance, Pharmacol Rev 57(3) (2005) 289-98.

[47] G. Milligan, G protein-coupled receptor hetero-dimerization: contribution to pharmacology and function, Br J Pharmacol 158(1) (2009) 5-14.

[48] N.J. Smith, G. Milligan, Allostery at g protein-coupled receptor homo- and heteromers: uncharted pharmacological landscapes, Pharmacol Rev 62(4) (2010) 701-25.

[49] M. Neri, S. Vanni, I. Tavernelli, U. Rothlisberger, Role of aggregation in rhodopsin signal transduction, Biochemistry 49(23) (2010) 4827-32.

[50] L.P. Pellissier, G. Barthet, F. Gaven, E. Cassier, E. Trinquet, J.P. Pin, P. Marin, A. Dumuis, J. Bockaert, J.L. Baneres, S. Claeysen, G protein activation by serotonin type 4

receptor dimers: evidence that turning on two protomers is more efficient, J Biol Chem 286(12) (2011) 9985-97.

[51] K.G. Harikumar, D. Wootten, D.I. Pinon, C. Koole, A.M. Ball, S.G. Furness, B. Graham, M. Dong, A. Christopoulos, L.J. Miller, P.M. Sexton, Glucagon-like peptide-1 receptor dimerization differentially regulates agonist signaling but does not affect small molecule allostery, Proc Natl Acad Sci U S A 109(45) (2012) 18607-12.

[52] J.L. Baneres, J. Parello, Structure-based analysis of GPCR function: evidence for a novel pentameric assembly between the dimeric leukotriene B4 receptor BLT1 and the G-protein, J Mol Biol 329(4) (2003) 815-29.

[53] S. Filipek, K.A. Krzysko, D. Fotiadis, Y. Liang, D.A. Saperstein, A. Engel, K. Palczewski, A concept for G protein activation by G protein-coupled receptor dimers: the transducin/rhodopsin interface, Photochem Photobiol Sci 3(6) (2004) 628-38.

[54] K. Herrick-Davis, E. Grinde, T.J. Harrigan, J.E. Mazurkiewicz, Inhibition of serotonin 5-hydroxytryptamine2c receptor function through heterodimerization: receptor dimers bind two molecules of ligand and one G-protein, J Biol Chem 280(48) (2005) 40144-51.

[55] B. Jastrzebska, T. Orban, M. Golczak, A. Engel, K. Palczewski, Asymmetry of the rhodopsin dimer in complex with transducin, Faseb J 27(4) (2013) 1572-84.

[56] W.M. Oldham, H.E. Hamm, Structural basis of function in heterotrimeric G proteins, Q Rev Biophys 39(2) (2006) 117-66.

[57] H.E. Hamm, D. Deretic, A. Arendt, P.A. Hargrave, B. Koenig, K.P. Hofmann, Site of G protein binding to rhodopsin mapped with synthetic peptides from the alpha subunit, Science 241(4867) (1988) 832-5.

[58] R. Herrmann, M. Heck, P. Henklein, K.P. Hofmann, O.P. Ernst, Signal transfer from GPCRs to G proteins: role of the G alpha N-terminal region in rhodopsin-transducin coupling, J Biol Chem 281(40) (2006) 30234-41.

[59] J.M. Taylor, G.G. Jacob-Mosier, R.G. Lawton, A.E. Remmers, R.R. Neubig, Binding of an alpha 2 adrenergic receptor third intracellular loop peptide to G beta and the amino terminus of G alpha, J Biol Chem 269(44) (1994) 27618-24.

[60] O.G. Kisselev, M.A. Downs, Rhodopsin-interacting surface of the transducin gamma subunit, Biochemistry 45(31) (2006) 9386-92.

[61] P. Scheerer, J.H. Park, P.W. Hildebrand, Y.J. Kim, N. Krauss, H.W. Choe, K.P. Hofmann, O.P. Ernst, Crystal structure of opsin in its G-protein-interacting conformation, Nature 455(7212) (2008) 497-502.

[62] S.G. Rasmussen, B.T. DeVree, Y. Zou, A.C. Kruse, K.Y. Chung, T.S. Kobilka, F.S. Thian, P.S. Chae, E. Pardon, D. Calinski, J.M. Mathiesen, S.T. Shah, J.A. Lyons, M. Caffrey, S.H. Gellman, J. Steyaert, G. Skiniotis, W.I. Weis, R.K. Sunahara, B.K. Kobilka, Crystal structure of the beta2 adrenergic receptor-Gs protein complex, Nature 477(7366) (2011) 549-55.

[63] S. Angers, A. Salahpour, E. Joly, S. Hilairet, D. Chelsky, M. Dennis, M. Bouvier, Detection of beta 2-adrenergic receptor dimerization in living cells using bioluminescence resonance energy transfer (BRET), Proc Natl Acad Sci U S A 97(7) (2000) 3684-9.

[64] D.G. Lambright, J. Sondek, A. Bohm, N.P. Skiba, H.E. Hamm, P.B. Sigler, The 2.0 A crystal structure of a heterotrimeric G protein., Nature 379(6563) (1996) 311-9.

[65] C.A. Johnston, D.P. Siderovski, Receptor-mediated activation of heterotrimeric G-proteins: current structural insights, Mol Pharmacol 72(2) (2007) 219-30.

[66] B. Jastrzebska, Y. Tsybovsky, K. Palczewski, Complexes between photoactivated rhodopsin and transducin: progress and questions, Biochem J 428(1) (2010) 1-10.

[67] Y. Hou, I. Azpiazu, A. Smrcka, N. Gautam, Selective role of G protein gamma subunits in receptor interaction, J Biol Chem 275(50) (2000) 38961-4.

[68] J.A. Hern, A.H. Baig, G.I. Mashanov, B. Birdsall, J.E. Corrie, S. Lazareno, J.E. Molloy, N.J. Birdsall, Formation and dissociation of M1 muscarinic receptor dimers seen by total internal reflection fluorescence imaging of single molecules, Proc Natl Acad Sci U S A 107(6) (2010) 2693-8.

[69] D. Calebiro, F. Rieken, J. Wagner, T. Sungkaworn, U. Zabel, A. Borzi, E. Cocucci, A. Zurn, M.J. Lohse, Single-molecule analysis of fluorescently labeled G-protein-coupled receptors reveals complexes with distinct dynamics and organization, Proc Natl Acad Sci U S A 110(2) (2013) 743-8.

LEGEND TO THE FIGURES

FIGURE 1. Predicted dimeric model of TPα.

Representation of the predicted dimeric interface of TPα seen from the intracellular side in a direction parallel to the membrane surface. For the sake of clarity only TM1 is shown. The side chains of the TM1 interface amino acids subjected to alanine substitutions are shown in gray.

FIGURE 2. [^{3}H]SQ29,548 binding curves of of TPα WT and DDM (A) and mutant surface expression in HEK293T cells (B).

Panel A. [^{3}H]SQ29,548 binding studies in HEK293T cells transiently expressing the WT (■) or DDM (□) of human TPα receptor. Mixed type curves were performed at 25°C with 30 min incubation. Binding is expressed as the ratio of bound ligand to total ligand concentrations (B/T, dimensionless) versus the logarithm of total unlabeled ligand concentration (Log T). Non-specific binding was calculated by computer as one of the unknown parameters of the model and was always <10% of total binding. Curves are computer generated from the simultaneous analysis of at least six experiments, each in duplicate. Values for K_d's are shown in Table 1. Panel B. Representative images of fluorescent signals emitted by donor (500 ng DNA HA-TPαDDM; green) and acceptor (500 ng DNA Myc- TPαDDM red) fluorochromes in two contiguous HEK293T cells expressing TPα DDM mutant.

FIGURE 3. Western blotting (A and B) and acceptor photobleaching FRET analysis (C and D) of HEK-293T cell transiently transfected with either TPα WT or DDM.

Panel A shows one representative analysis of eight independent western blots. Histograms in Panel B show the densitometric analysis of bands referred to mono- and dimeric Myc-tagged WT and DDM mutant receptors performed with 'gel analizer' ImageJ' plugin. The results are expressed as relative over total intensities of each single lane. Comparison of multiple groups performed using one-way ANOVA followed by Bonferroni's Multiple Comparison Test reveals a statistically significant decrease in the dimeric and an increase in the monomeric form of DDM compared to TPα WT (***$p<0.001$). Error bars represent the means ± SE of at least three independent experiments. Panel C and D. HEK293T cells co-transfected with TPα WT or DDM mutant, tagged with two different epitopes, were labeled in vivo with the corresponding anti-tag antibodies. After fixation cells were subjected to indirect immunofluorescence with Alexa Fluor 488- (donor fluorochrome) or 555 (acceptor fluorochrome)-conjugated secondary antibodies and imaged with laser scanning confocal microscopy. Panel C shows representative images of donor (2.5 ng DNA HA-TPα; green) and acceptor (2.5 ng DNA Myc-TPα; red) fluorescence signals to clarify how regions of interest (ROIs) were selected for the analysis. Images show two contiguous HEK293T cells expressing wild type HA-TPα and Myc-TPα pairs before and after laser-induced photobleaching of acceptor fluorescence in the defined ROIs (dotted lines). Panel D show the quantitation of average percent donor and acceptor fluorescence intensities of WT and DDM mutant HA-TPα and Myc-TPα, respectively, normalized for unbleached 'sentinel' plasma membrane ROIs (broken lines in panel A). No statistically significant differences were observed in acceptor recovery (i.e. FRET signal) comparing the three different levels of expression transfected (● 500 ng, ■ 5 ng, ▲ 0.5 ng cDNA). The decrease in WT and DDM Myc-TPα acceptor signals are not significantly different. Statistical analysis of

immunofluorescence data was performed using one-way ANOVA repeated measurements with one grouping factor for all frames. Data are expressed as the means ± SE of 10 different fields from three independent experiments. Scale bar = 10μm.

FIGURE 4. Basal activity in HEK293T cells transiently expressing TPα WT or DDM in the absence and presence of Gαq overexpression.

Total IP accumulation in basal conditions (white bars) and in the presence (black bars) of Gαq overexpression (TPα and Gαq plasmids were added in a 1:5 ratio (5xGq). Data are expressed as dpm/well. Error bars represent the means ± SE of at least three independent experiments each performed in duplicates or triplicates.

FIGURE 5. IP dose-response curves in HEK293T cells transiently expressing equal amounts of the WT or DDM of human TPα receptor.

Agonist-induced total IP accumulation in HEK293T cells was measured after incubation in the absence (basal) or presence of increasing concentrations of the indicated agonists for 30 min. Panel A and B. Agonist-induced effects (□ U46619, ○ I-BOP, ◆ 8-isoPGE$_2$, △ 8-iso-PGF$_{2\alpha}$). Panels C and D. Antagonist induced-effects (■ SQ29,548, ▼ Ramatroban) in the presence of 1μM U46619. Data are expressed as fold increase over basal. Curves are computer-generated from the simultaneous analysis of at least three independent experiments each performed in duplicates or triplicates. Error bars represent the means ± SE. Values for EC$_{50}$'s and significant differences from WT are shown in Table 2.

FIGURE 6. IP dose-response curves (A) and acceptor photobleaching FRET analysis (B) of HEK293T transiently expressing WT, DDM or TPtrunc of human TPα receptor.

Panel A. Agonist-induced total IP accumulation was measured after incubation in the presence of increasing concentrations of U46619 in HEK293T cells transfected with (■) TPα WT, (□) DDM, (●) TPα WT + TPtrunc, (○) TPα WT + TPtrunc TM1 and (*) TPtrun alone. TPtrunc represent represents the truncated form of TP coding only for the N terminal and TM1 regions (Ser57-Stop), while TPtrunc TM1 represents the truncated form of TP carrying the same eight mutations as DDM. Data are expressed as fold increase over basal. Curves are computer-generated from the simultaneous analysis of at least three independent experiments each performed in duplicates or triplicates. Error bars represent the means ± SE. Panel B. The graph show the quantitation of average percent donor and acceptor fluorescence intensities in HEK293T transfected with TPα couples (■ WT/WT, ● WT/TPtrunc and ▲ WT/DDM, respectively) with a 1:1 DNA ratio, normalized for unbleached 'sentinel' plasma membrane ROIs in acceptor photobleaching FRET assays. No statistically significant differences were observed in acceptor recovery (i.e. FRET signal) comparing the WT/WT and WT/TPtrunc samples while, as previously observed, WT/DDM couple do not show any significant FRET signals. Statistical analysis data was performed using one-way ANOVA repeated measurements with one grouping factor for all frames. Data are expressed as the means ± SE of 10 different fields from three independent experiments.

FIGURE 7. Ligand binding profile of WT and DDM of human TPα receptor

Agonist binding studies in HEK293T cells transiently expressing the WT (A and C) or DDM (B and D) of human TPα receptor. For each construct, cold SQ29,548(■), U46619(□), I-BOP(○), 8-isoPGE$_2$(◆) or 8-isoPGF2α(△) or PTA2(▲) were used in competition against 1

nM [^{3}H]SQ29,548. Mixed type curves and heterologous competition curves were performed at 25°C with 30 min incubation. Binding is expressed as the ratio of bound ligand to total ligand concentrations (B/T, dimensionless) versus the logarithm of total unlabeled ligand concentration (Log T). Non-specific binding was calculated by computer as one of the unknown parameters of the model and was always <10% of total binding. Curves are computer generated from the simultaneous analysis of at least three independent mixed-type and heterologous competition experiments, each in duplicate. Values for K_i's are shown in Table 3.

FIGURE 8. TPα receptor expression in human platelets.

Total TP receptor expression was assessed in platelets from healthy donors (HD) or a patient expressing the W29C-TPα (W29C) variant by immunoblotting with a receptor specific antibody. Panel A. Representative blot of four independent experiments. Equal loading was confirmed by assessing tubulin levels (lower blot). Panel B. Densitometric analysis of bands referred to as monomer, dimer and oligomer as assessed using ImageJ software. Data are expressed as band density (band density - background). Comparison of multiple groups performed using one-way ANOVA followed by Bonferroni's Multiple Comparison Test.

FIGURE 9. Acceptor photobleaching FRET analysis of HEK293T cells transiently expressing WT-WT, WT-W29C or WT-N42S TPα pairs.

HEK293T cells co-transfected with different TPα pairs, tagged with HA and FLAG epitopes, were in vivo labeled with the corresponding anti-tag antibodies. After fixation, cells were subjected to indirect immunofluorescence with Alexa Fluor 488- (donor fluorochrome) or 555 (acceptor fluorochrome)-conjugated secondary antibodies and imaged with laser

scanning confocal microscopy. Panel A shows representative images of fluorescent signals emitted by donor (green) and acceptor (red) fluorochromes in two contiguous HEK293T cells expressing WT FLAG-TPα and HA-TPα pair before and after laser-induced photobleaching of acceptor fluorescence in a defined plasma membrane region of interest (ROI; dotted line). Panel B shows the histogram of the quantitation of average percent donor fluorescence intensities of WT-WT, WT-N42S or WT-W29C TPα pairs, normalized for unbleached 'sentinel' plasma membrane ROIs after laser-induced photobleaching of acceptor fluorescence. Statistical analysis of immunofluorescence data was performed using one-way ANOVA repeated measurements with one grouping factor (**$p < 0.01$; n=40, 4 independent experiments). Data are expressed as the means ± SE of ten different fields from four independent experiments. Scale bar: 10 μM.

FIGURE 10. IP dose-response curves in HEK293T cells transiently expressing equal amounts of the WT, W29C or N42S mutants of human TPα receptor.

Agonist-induced total IP accumulation in HEK293T cells was measured after incubation in the absence (basal) or presence of increasing concentrations of the indicated agonists for 30 min (Panel A ■,□ U46619, ●,❍ I-BOP; Panel B ◆◇ 8-isoPGE$_2$, ▲,△ 8-iso-PGF$_{2\alpha}$). Data are expressed as fold increase over basal. Curves are computer-generated from the simultaneous analysis of at least three independent experiments each performed in duplicates or triplicates. Error bars represent the means ± SE.

Figure 11. BRET^2 measurement of $G\alpha_q\beta_1\gamma_2$ complex activation in HEK293T cells expressing equal amounts of WT, DDM, W29C or N42S mutants of human TPα receptor.

A and B. BRET was measured in HEK293T cells co-expressing $G\alpha_q$-Rluc8 together with GFP^{10}-$G\gamma_2$ and $G\beta_1$ in the presence of WT (■), DDM (□) N42S (△) or W29C (▽) mutants of the human TPα receptor and stimulated with increasing concentrations of U46619 for 2 min. Results are indicated as BRET ligand effect that as been calculated as the differences in the BRET signal measured in the presence and the absence of the agonist, and are expressed as the mean value ± SE of at least three independent determinations. Values for EC_{50}'s and significant differences from WT are shown in Table 4.

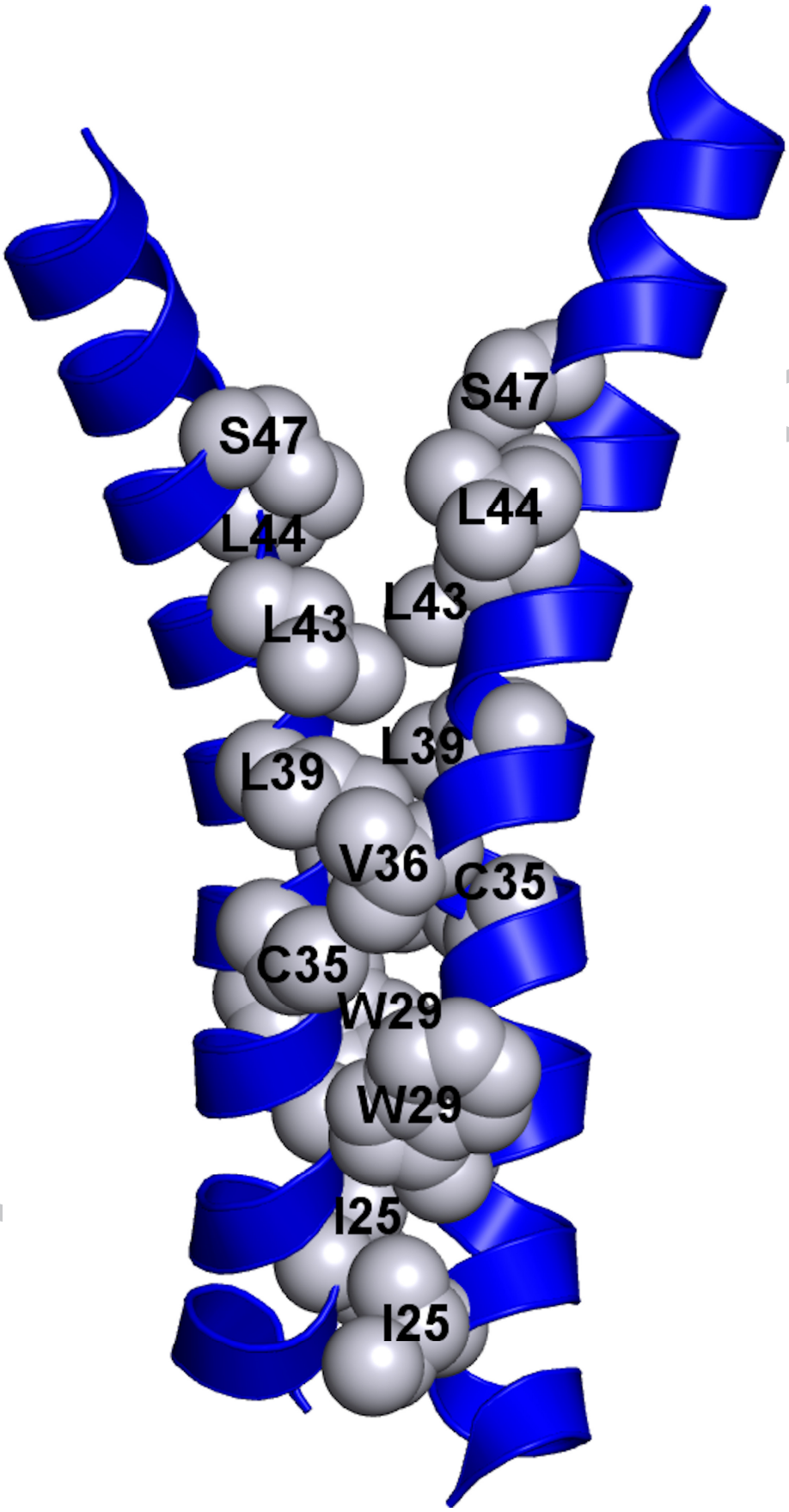

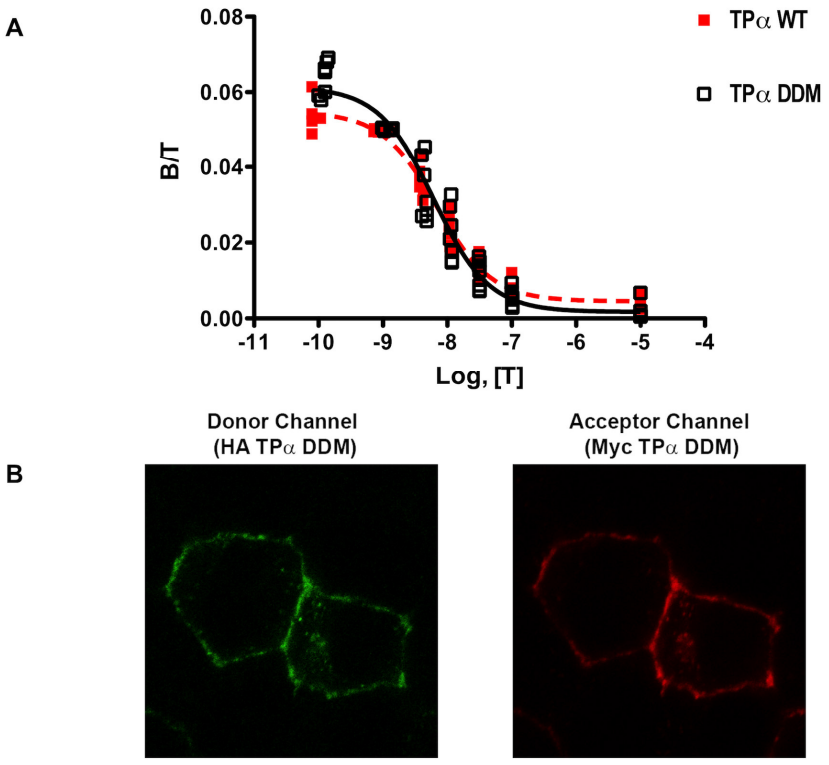

Fig. 2

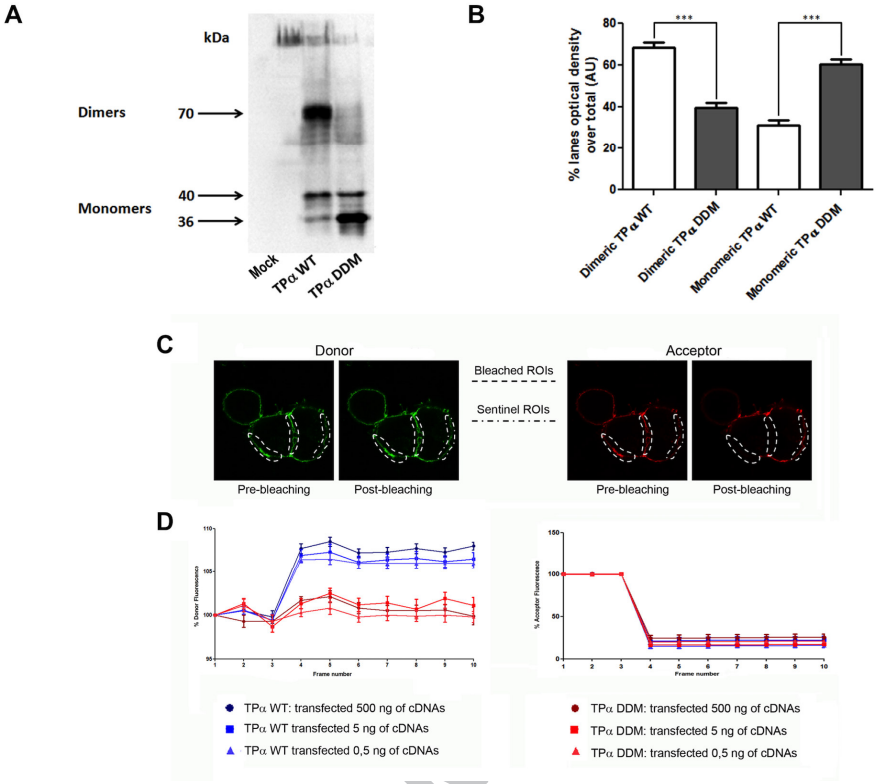

Fig. 3

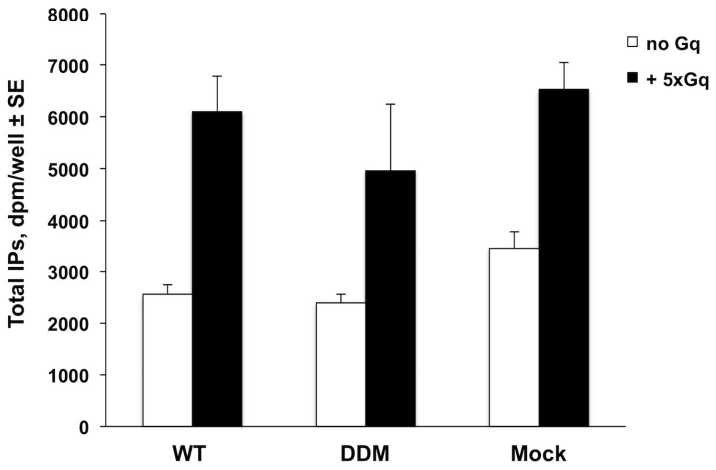

Fig. 4

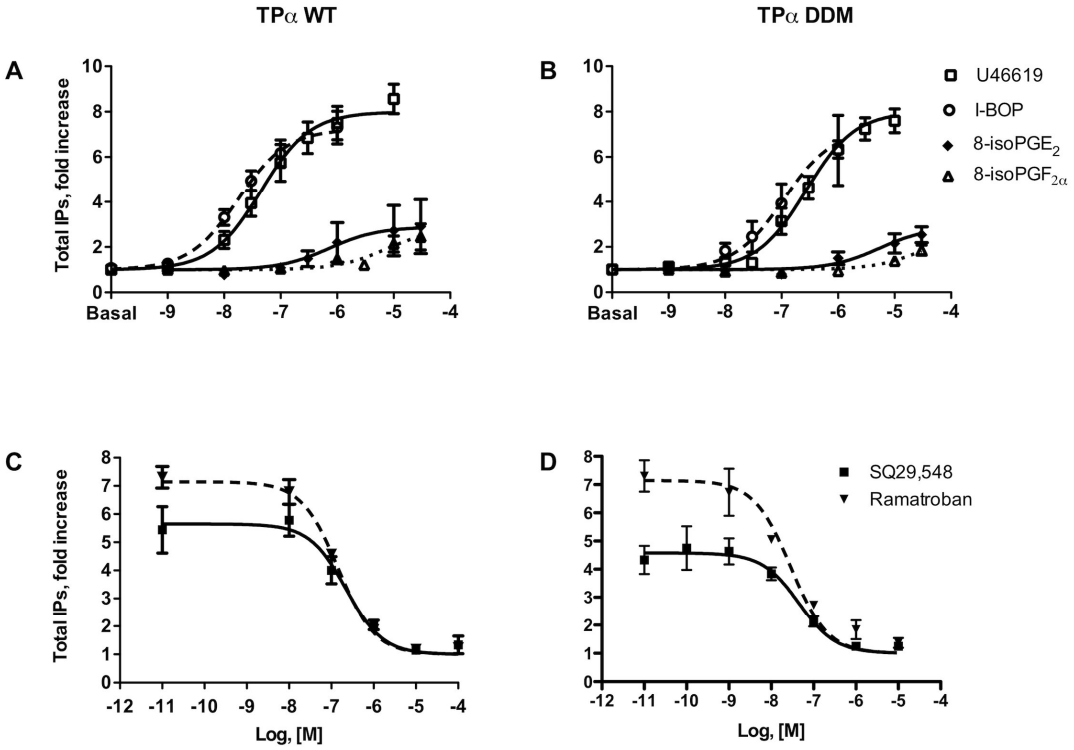

Fig. 5

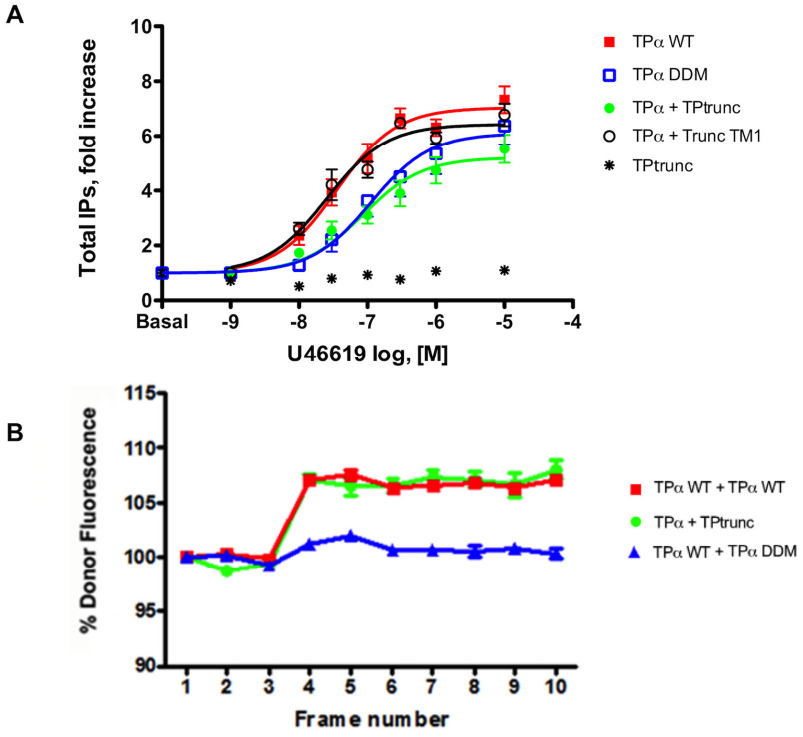

Fig. 6

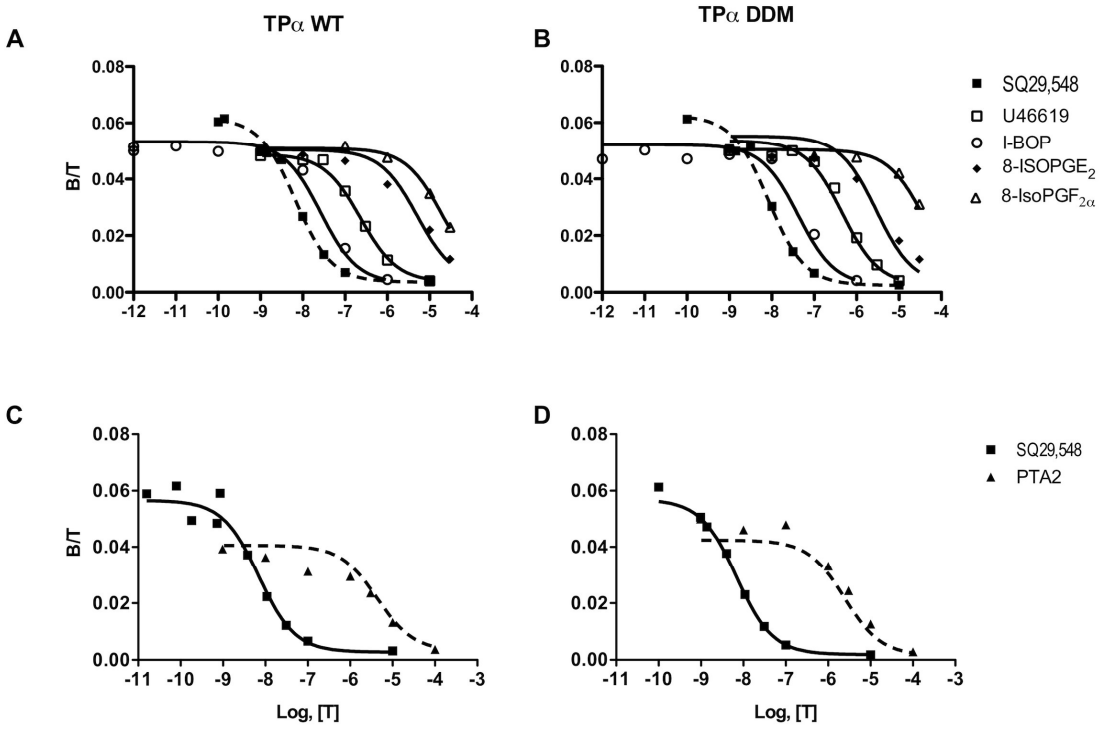

Fig. 7

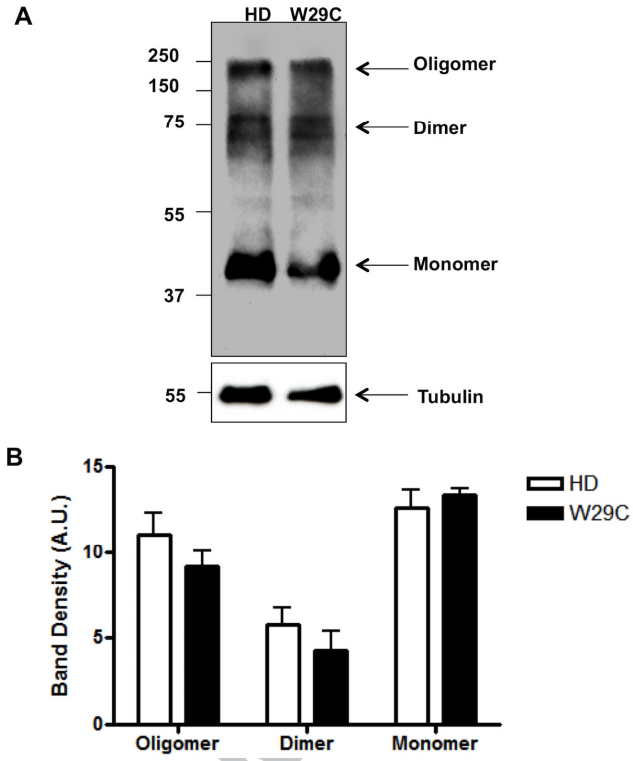

Fig. 8

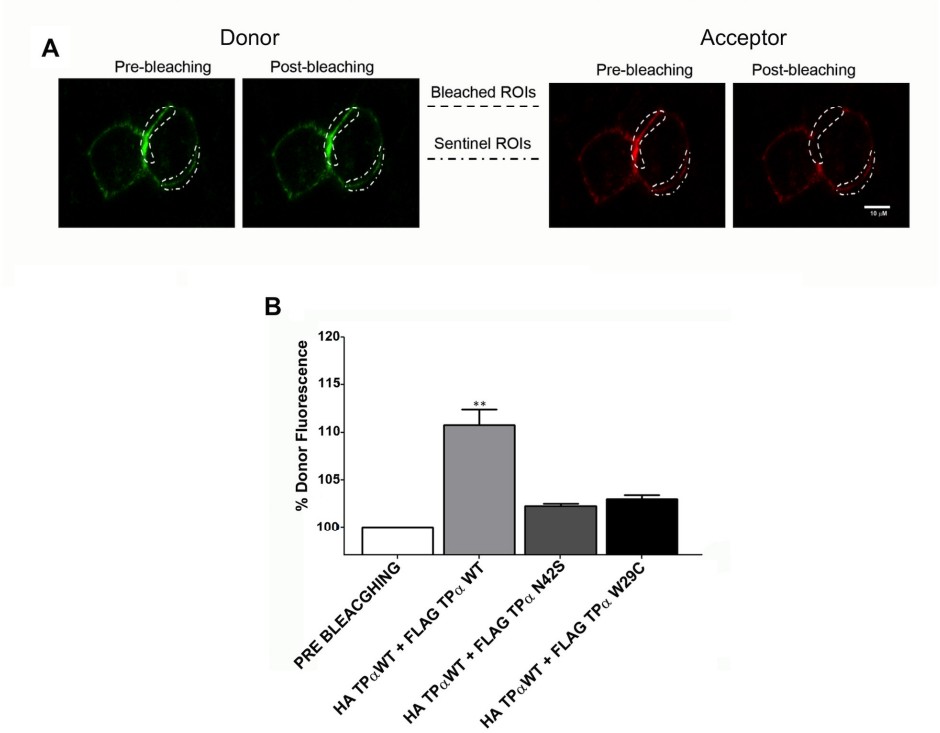

Fig. 9

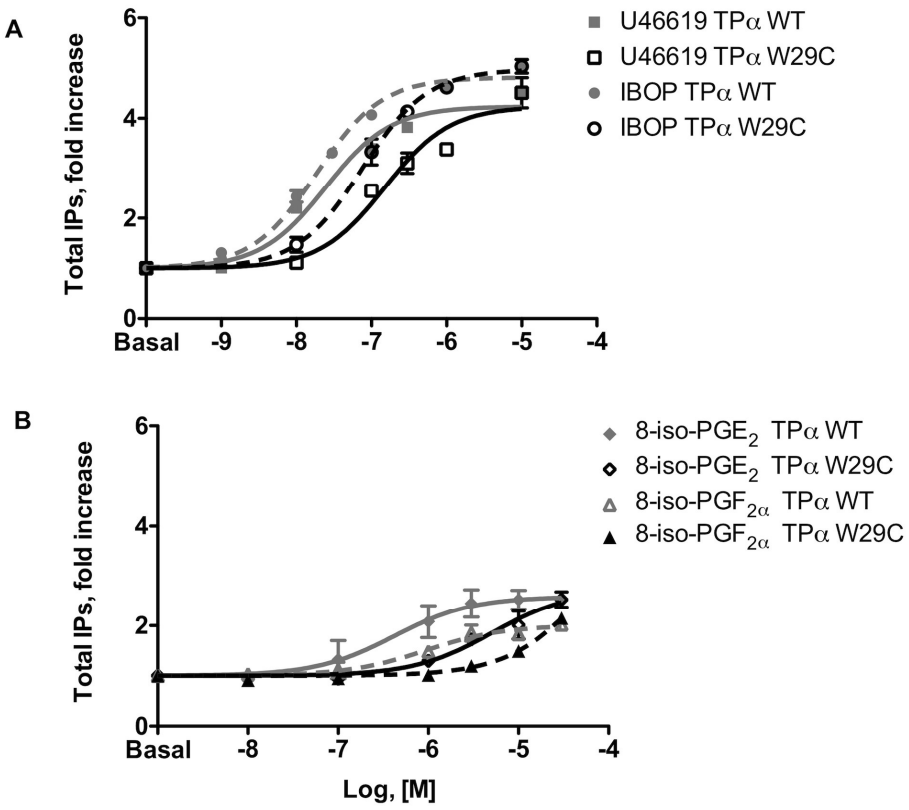

Fig. 10

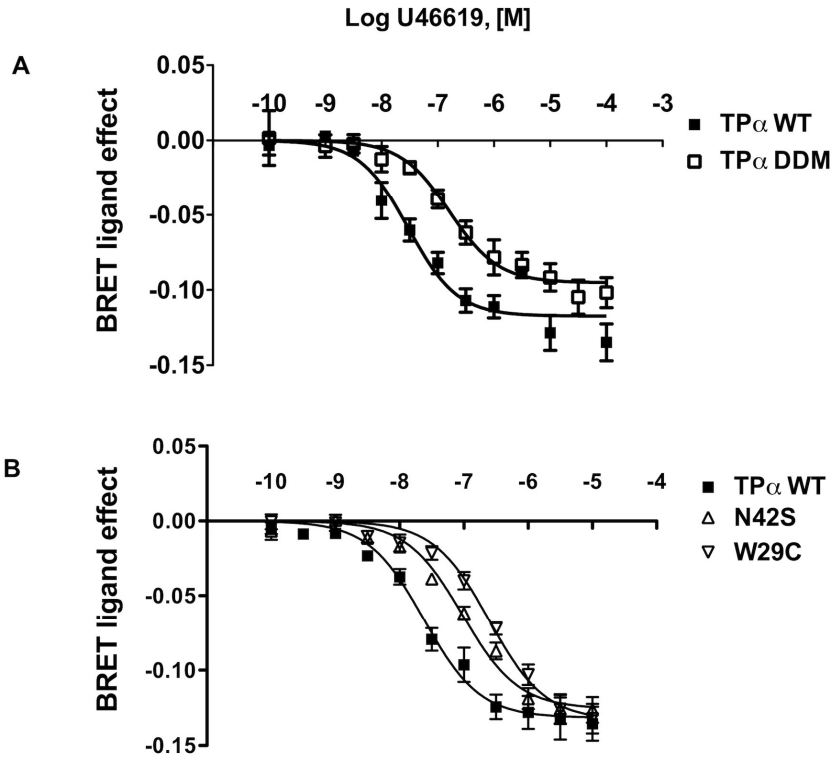

Fig. 11

Table 1. Binding affinities of [^{3}H]SQ29,548 in HEK293T cells transiently expressing the WT or mutant human TP receptors. Binding affinities and capacities were obtained by simultaneous analysis of at least six independent mixed-type experiments, each performed in duplicate (see Materials and Methods).

Receptor	**K_d, nM ± %CV**	**B_{max}, pmol/mg prot ± %CV**
WT	6.1 ± 30	0.85 ± 47
DDM	7.6 ± 28	1.3 ± 38

Table 2. Total IP dose-response parameters for different agonists in HEK293T cells transiently expressing the WT or DDM receptors. Values of EC_{50}'s and E_{max}'s were obtained by simultaneous analysis with GraphPad Prism (see Materials and Methods) of at least three independent experiments each performed in duplicates or triplicates.

	WT		**DDM**	
Agonist	**EC_{50}, nM ± %CV**	**E_{max}, fold increase ± %CV**	**EC_{50}, nM ± %CV**	**E_{max}, fold increase ± %CV**
U46619	45 ± 31	8.1 ± 4.5	270 ± 23**	7.7 ± 4
I-BOP	17.6 ± 29	7.3 ± 5	110 ± 54**	6.7 ± 12
8-isoPGE$_2$	702 ± 82	2.8 ± 14§	5400 ± 85**	2.8 ± 14§
8-isoPGF$_{2\alpha}$	5361 ± 93	2.7 ± 13§	32400 ± 89**	2.7 ± 13§

** $p < 0.01$ vs. WT

§ shared parameters

Table 3. Agonist affinities for the receptor binding site labeled by [^{3}H]SQ29,548 in HEK293T cells transiently expressing the WT or the DDM receptors. K_i values were obtained by simultaneous analysis of at least three independent experiments analyzed with GraphPad Prism implemented with the LIGAND model (see Materials and Methods).

	WT	**DDM**
Agonist	**K_i, nM ± %CV**	**K_i, nM ± %CV**
U46619	199 ± 13	404 ± 24
I-BOP	23 ± 30	37 ± 30
8-isoPGE$_2$	4296 ± 35	2838 ± 41
8-isoPGF$_{2\alpha}$	16900 ± 38	34360 ± 64

Table 4. BRET concentration-response parameters for U46619-induced G protein activation in HEK293T cells transiently expressing the WT or different TPα receptor mutants. Values of EC_{50}'s and E_{max}'s were obtained by simultaneous analysis with GraphPad Prism (see Materials and Methods) of at least three independent experiments each performed in triplicates.

	EC_{50}, nM ± %CV	**E_{max}, ± %CV**
WT	29.9 ± 28	-0.12 ± 4
DDM	161 ± 36**	-0.095 ± 5
N42S	94.5 ± 15**	-0.13 ± 3
W29C	247 ± 19**	-0.13 ± 4

** p< 0.01 vs. WT

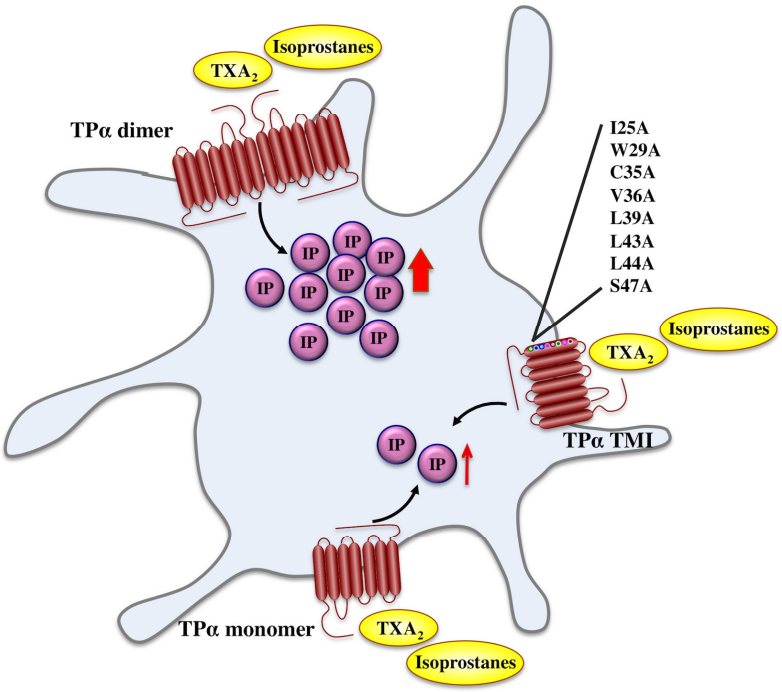

Graphical abstract